

Chapter 2

Control and Management of PV Integrated Charging Facilities for PEVs

Preetham Goli and Wajiha Shireen

Abstract The ongoing research in the field of plug-in electric vehicles (PEVs) and the growing global awareness for a pollution free environment, will lead to an increase in the number of PEVs in the near future. The proliferation of these PEVs will add stress to the already overloaded power grid creating new challenges for the distribution network. To mitigate this issue several researchers have proposed the idea of charging PEVs using renewables coupled with smart charging strategies. This chapter reviews the current literature on the state of the art infrastructure proposed for PEV charging facilities integrated with photovoltaic system. The proposed control algorithms, various smart charging techniques and different power electronic topologies for photovoltaic charging facilities (PCFs) are reviewed. Studies assessing the ability of photovoltaic charging stations to minimize the loading on distribution transformers are assessed. Finally, a simple and unique energy management algorithm for a PV based workplace charging facility based on dc link voltage sensing is presented. The power needed to charge the plug-in electric vehicles comes from grid-connected photovoltaic (PV) generation or the utility or both. The efficacy of the proposed algorithm is validated through simulation and experimental results.

Keywords Plug-in electric vehicles (PEVs) • Photovoltaic charging facility (PCF) • Distribution network

P. Goli (✉)

Department of Electrical and Computer Engineering, University of Houston, Houston, USA
e-mail: pgoli2@central.uh.edu; preethamgoli@gmail.com

W. Shireen

Department of Electrical and Computer Engineering, Department of Engineering Technology, University of Houston, Houston, USA
e-mail: wshireen@central.uh.edu

2.1 Introduction

With the growing global awareness for a pollution free environment, rising energy costs, PEVs are being introduced by many automotive makers. It is known that if 25 % of the 176 million fleets of light vehicles in U.S were converted to PEVs, it will rival the entire U.S power generation capacity [1]. The proliferation in PEVs requires charging stations to fulfil their battery requirements. Though PEVs are being marketed with the goal of minimizing the pollution from automobiles, the energy requirements for charging the batteries is still met by power generated by fossil fuel sources. Hence many researchers have proposed the idea of charging PEVs using renewable energy sources like wind and photovoltaic. Many pilot projects are also underway to charge PEVs from solar photovoltaic system [2–5]. Charging stations based on wind power is still in the nascent stages though few ventures have been announced [6]. Due to the social and economic benefits, research on charging stations featuring photovoltaic system has attracted researchers around the world.

Using solar power to charge batteries is not a new idea. It is a reliable source for charging light duty electric vehicles such as golf carts, scooters and airport utility vehicles [7]. Large-scale deployment of photovoltaic chargers in a parking lot is analysed in [8]. A 2.1 kW photovoltaic charging station integrated with the utility at Santa Monica is described in [9]. An experimental control strategy for electric vehicle charging system composed of photovoltaic array, emulated power grid and programmable dc electronic load representing lithium ion battery emulator is presented in [10]. PV parking lot charging and other business models to charge PEVs with solar energy are discussed in [11]. Economics of PV powered workplace charging station has been studied in [12, 13]. The analysis shows the feasibility of a PV based workplace parking garage with benefits to the vehicle owner as compared to home charging, such that the garage owner will get the payback of installations and maintenance cost and profit within the lifetime of the PV panels. According to [13] integrating a solar collector into a parking lot would result in a much more rapid payback-period, encouraging widespread installation of solar capacity. Reference [14] describes how smart control strategies can help PEVs and PV to integrate with the present electricity systems. Co-benefits of large scale deployment of PEVs and PV systems has been studied in [15]. The study concludes that PV provides a potential source of midday generation capacity for PEVs, while PEVs provide a dispatchable load for low value or otherwise unusable PV generation during periods of low demand (particularly in the spring).

As per the National household travel survey vehicles are parked for at least 5 h in workplaces [16]. Hence these places are favorable for developing charging station infrastructure but this would lead to serious overloading issues at the distribution level. Since upgrading of transformers is an expensive option for the utilities, this issue needs close attention as the PEV penetration increases. Several papers have been published to address the overloading of distribution transformers while charging the PEVs [17–19]. Nevertheless, not much study has been reported to be

Table 2.1 PV characteristics [23]

PV type	Module price (\$/W _p)	Efficiency (%)	Peak energy (W _p)	Total cost of PV (\$)
Crystalline silicon	2.14	22	264	565
Polycrystalline silicon	1.74	15.5	186	324
Thin film	0.93	12	144	134

tightly related to the case of reducing the loading on distribution transformers using a photovoltaic system. Though few papers exist in the literature, they are mostly confined to residential distribution networks [20, 21]. There is plenty of parking area in the U.S—a reasonable fraction of which is suitable for PV installation. This chapter reviews the current literature on the state of the art infrastructure proposed for PEV charging facilities integrated with photovoltaic system. The proposed control algorithms, various smart charging techniques and the economic benefits of photovoltaic charging facilities (PCFs) are reviewed. Various power electronic topologies, control algorithms and charging strategies will be discussed. It will be shown that a network of PCFs will accelerate the deployment of PEVs through economic and environmental benefits to the utilities and vehicle owners. The impact of grid connected photovoltaic system on the utility distribution networks is analyzed. The suitability of using PV power for charging PEVs is accessed in this chapter.

Determining the size and type of PV panel is an important consideration for a solar carport. Few papers [22, 23] have recommended the use of monocrystalline silicon as the most cost-effective solar cell type for PV charging facilities. Table 2.1 shows the PV characteristics of various modules, the peak energy produced and the total cost of the PV module. The PV panel can be sized by taking the best and worst months into consideration. As described in [24], the initial cost of the PV panel would be \$20,000 when it is designed based on the worst month of the year and \$10,000 when it is designed based on the best month of the year. However, for the first case, surplus energy can be injected into the grid, to balance the final cost.

2.2 Impact of PEV Charging on the Distribution System

Large-scale penetration of PEVs can have a detrimental and destabilizing effect on the electric power grid. With the variation in demand, the production of power can vary significantly. Variation in charging time of PEVs can result in distinct differences in fuels and generating technologies [25]. Figure 2.1 illustrates the impact of charging one million PEVs on the Virginia—Carolinas electric grid in 2018 on the various generation technologies. As shown in Fig. 2.1, at low specific power and late in the evening, coal was the major fuel used, while charging more heavily

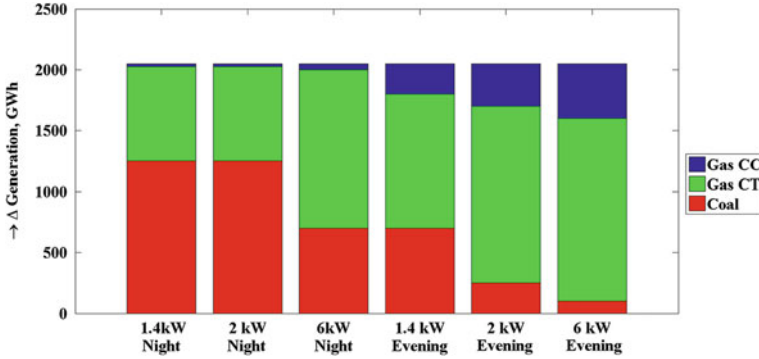


Fig. 2.1 Generation shares by plant type for PEV charging level and timing [25]

during peak times led to more use of combustion turbines and combined cycle plants. Since the initial deployment of PEVs is assumed to be clustered to a particular neighborhood, many authors have focused their research on the study of distribution transformer impacts. Depending upon the time, place of vehicle charging, various charging methods and the charging power levels there could be several ramifications on the distribution network. Various analytical techniques and different simulation tools were employed by several authors to estimate the transformers loss-of-life, average lifetime and harmonic losses. The percentage of transformers loss-of-life and average lifetime are important factors to be considered while studying the charging behavior of PEVs on future distribution system. High penetration of PEVs in the future will increase the loss-of-life factor of distribution transformers [26–29].

The impact of controlled and uncontrolled charging of PEVs on the average lifetime of a transformer is described in [24, 26]. As per [24], the average lifetime of a transformer is reduced by 4–20 % under uncontrolled charging for a PEV penetration of 10 %. At 50 % penetration of PEVs, the average lifetime is reduced by 200–300 % with uncontrolled charging. On the other hand controlled charging increases the lifetime by 100–200 % with respect to uncontrolled charging for 50 % penetration of PEVs. Plug-in electric vehicle charging rates can have a significant impact on the lifetime of a transformer [24, 25]. Table 2.2 summarizes the sensitivity of transformer lifetime to different charging rates (3.6 and 7.7 kW) under controlled and uncontrolled charging for various levels of PEV penetration. As expected, transformer life degradation is exacerbated when the charging rate is increased from 3.6 to 7.7 kW.

The percentage of transformers loss-of-life can be minimized through distributed charging and controlled off-peak charging which requires coordination among utilities, customers and charging stations. Simulation results in [17] show that distributing the load profile of the battery charging helps to minimize the distribution transformer loss-of-life. Power management of the PEV battery charge profile can help manage the loss-of-life of the distribution transformer. Controlled

Table 2.2 Impact of charging PEVs [27]

Charger rating	3.6 kW			7.7 kW		
Charge type	Uncontrolled (years)		Controlled (years)	Uncontrolled (years)		Controlled (years)
PEV penetra- tion (%)	Minimum lifetime	Average lifetime	Minimum lifetime	Minimum lifetime	Average lifetime	Minimum lifetime
10	29.2	61.1	32.7	27	49.8	34.1
25	26.8	37.4	25.7	16.8	36.5	33.3
50	12.2	38.9	10.7	11.2	24.3	29.9
75	16	31.4	11.7	5.8	14.5	42.9
100	8.3	18.4	12.8	2.3	10.5	26.8
						38.8

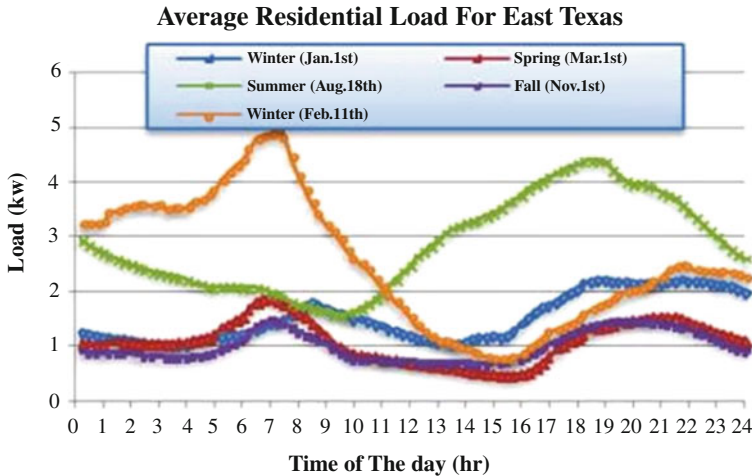


Fig. 2.2 15 min interval data of average residential individual customer in East Texas [26]

off-peak charging can shift PEVs charging load to an off-peak time. Usually charging PEVs at night time is proposed as the best way to mitigate the loss-of-life issues of distribution transformers. However, PEVs can also introduce a new peak or near peak in early off-peak time. Generally, the impact of extra load on transformers in summer is much greater than that in winter. However, some winter mornings with peak load may be an exception. Charging from midnight through early morning in those days may exert strong impact on transformers. Figure 2.2 describes this effect by taking the average residential load for East Texas into consideration. As shown in the figure for a particular day in winter, February 11th, the load consumed in the early morning is higher than that in summer days. Therefore, it is not always appropriate to charge electric vehicles at 1 am in those days. The required control strategy should depend on the actual load profile in a particular area for a particular time period.

2.3 Mitigating the Impact of PEV Charging on the Distribution System

To mitigate the issue of transformer loss-of-life due to PEV charging, integration of renewables like rooftop PV systems into the existing power grid has been proposed. In [30], a case study for the year 2030 was built based on demand increase, forecasted PEV and DG units. The results showed that PEV battery charging would prove onerous for the constraints studied. DG penetration would be able to provide support for PEV battery charging but PEV battery charging management would be necessary to minimize the impact in order to reach high levels of PEV penetration.

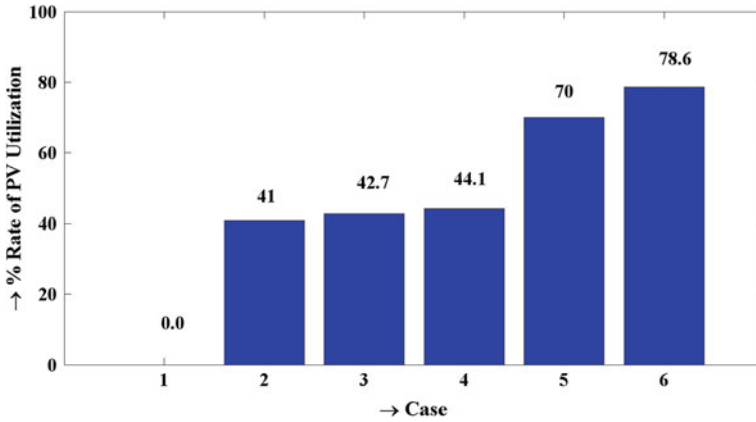


Fig. 2.3 The rate of PV utilization [32]

The possibility of smoothing out the load variance in a household microgrid by regulating the charging patterns of family PEVs is investigated in [31]. A case study is presented, which demonstrates that, by regulating the charging profiles of the PEVs, the variance of load power can be dramatically reduced. Integration of residential PV system with PEVs is studied in [32]. A residential PV system was simulated for various charging schemes of PEVs and the results are shown in Fig. 2.3. Several cases with different combinations of PV, PEV, V2H (Vehicle to Home i.e. discharge of PEV) and various charging schemes were analyzed. Case 1 describes a residential facility without PV and PEV. Case 2 describes a residential facility integrated with rooftop PV system without PEV. Therefore, these 2 cases analyze the effects of using PV while using gasoline vehicles instead of PEVs. Case 3 represents a residential facility with PV and PEV without V2H capabilities. Cases 4–6 have all the facilities (i.e. PV, PEV and V2H capabilities) but their charge-discharge schemes are different. As shown in Fig. 2.3 the local consumption rate of PV output increased by 1.7 % when gasoline vehicles are replaced with PEVs. On the other hand the rate of PV utilization increased by 8.6 % when the charging scheme changed from fixed (fixed target of SOC) to variable (variable target value of SOC).

The integration of PV rooftop in PCFs can relieve the burden on the distribution networks, by reducing the effective load seen by the distribution grid peak charging, as well as supplying power to the grid when excess power is generated by PV rooftops. A PV parking lot for PEVs is proposed in [33], in which the PEVs can be charged from the PV source as well as the distribution grid. Mathematical models are developed to estimate the electric power capacity for PV parking lot. An evaluation of impacts resulting from expected scenarios are performed through stochastic sequential simulations of the distribution system with load and PV generation in [34]. Figure 2.4 shows the LOL (loss-of-life) experienced at a particular distribution transformer, for change in stochastic load and PV generation

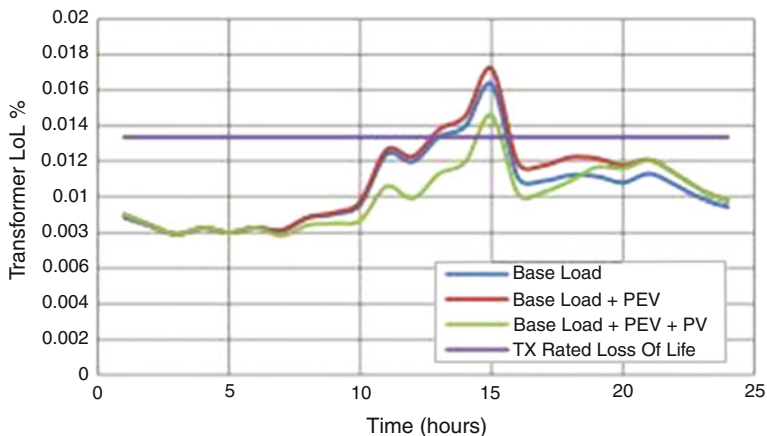


Fig. 2.4 Stochastic distribution transformer loss of life [34]

units. It is evident from the figure that rooftop PV coupled with PEVs can reduce LOL of the distribution transformer. These studies have shown that PV generation coupled with PEV charging can delay and reduce the temperature rise of distribution transformers.

2.4 Proposed Architectures for PV Based PEV Charging Facilities

The charging units for PEVs can be either on-board or off-board. In case of an off-board charger, the charger is an external unit while in the case of an on-board charger it is a component of the vehicle. On-board chargers are supplied with ac power and they consist of an AC/DC rectifier, DC/DC boost converter for power factor correction and a DC/DC converter to charge the battery as shown in Fig. 2.5. Currently AC charging is being employed to charge PEVs by means of on-board chargers. The major drawback of this technology is that it does not support fast charging as it is required to increase the power capability of the on-board charger thereby increasing the cost and weight of the PEV. Hence to support fast charging

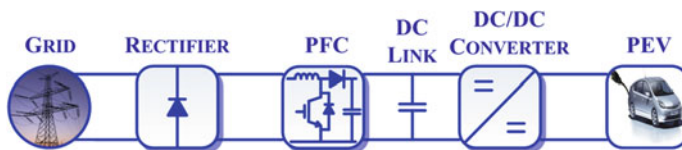


Fig. 2.5 Conventional PEV charger

of PEVs off-board chargers are proposed which directly supply dc power to the PEV charging inlet. It is to be noted that in case of an off-board charger the entire power conversion (AC/DC) takes place in an external unit and therefore it is feasible to increase the ratings of the power converters in order to support fast charging.

AC system is being used since years for power distribution and there are well developed infrastructure-standards and technologies. DC system on the other hand has many advantages, starting with the fact that overall efficiency of the system could be higher and it facilitates the integration of renewable energy sources with fewer power converters. Since PV arrays generate dc power, a charging facility featuring PV power facilitates the charging of PEVs from a dc bus which is more effective, economical and efficient since it does not involve more power conversion stages unlike AC charging. Various methods have been proposed for integrating PEV chargers within a photovoltaic system. Several power electronic topologies for a PCF have been proposed in the literature based on the type and the number of converters which are classified as:

- A. Centralized architecture
- B. Distributed architecture
- C. Single stage conversion with Z-converter

A. Centralized architecture

Detailed block diagram representing the centralized architecture is shown in Fig. 2.6. It consists of a central DC/DC boost converter which performs the function of maximum power point tracking. The DC/DC chargers are integrated with the PV charging facility at the dc link. Multiple PEVs can be charged by increasing the corresponding ratings of PV panels and the associated power converters. Each parking spot must have a dedicated DC/DC buck converter which is connected to the dc link. This configuration is suitable for charging stations in the range of several kilowatts. It is applicable for charging vehicles like golf carts, campus utility vehicles etc. which commute for very short distances with low battery capacities. Battery switch station powered by PV is a good candidate for adopting centralized architecture. But this kind of configuration does not support fast charging since

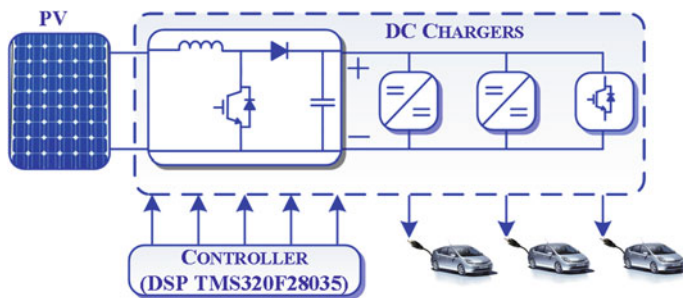


Fig. 2.6 Centralized architecture

installation of a very high power DC/DC converter is very expensive and it is vulnerable to single fault shutdown.

B. Distributed Architecture

Presence of DC/DC converters with high power ratings is an important criterion for fast charging of PEVs. This can be achieved economically through distributed architecture as shown in Fig. 2.7. In this case several strings of PV panels are connected in series. Each parking spot has a dedicated PV panel to support the charging of PEV and each string of PV panels is interfaced with their own DC/DC converter and shares a common dc bus, which connects to an AC utility grid through a bi-directional DC/AC converter. The DC/DC battery chargers are connected to the dc bus. Each parking spot requires an individual DC/DC converter to charge the PEVs. The proposed architecture is suitable for installation at places such as workplace, universities, shopping malls etc. where the demand of PEVs and their duration of stay in the parking lots are highly probabilistic in nature. It is more reliable since the PEVs can be charged from the grid during the periods of low insolation or cloudy weather. Also, it is important to note that the extra energy generated by PV can be injected into grid, which can be used to balance the PV costs.

A PCF requires constant power from the PV or the grid to meet the high demand of PEVs. The reliability of a PCF can be improved by including an energy storage unit such as a battery bank, ultra capacitor, fuel cell etc. For instance in [35] the power generated by roof top photovoltaic system is stored in VRLA (valve-regulated lead-acid) batteries and fuel cells in a PEV docking station. The PEVs arriving

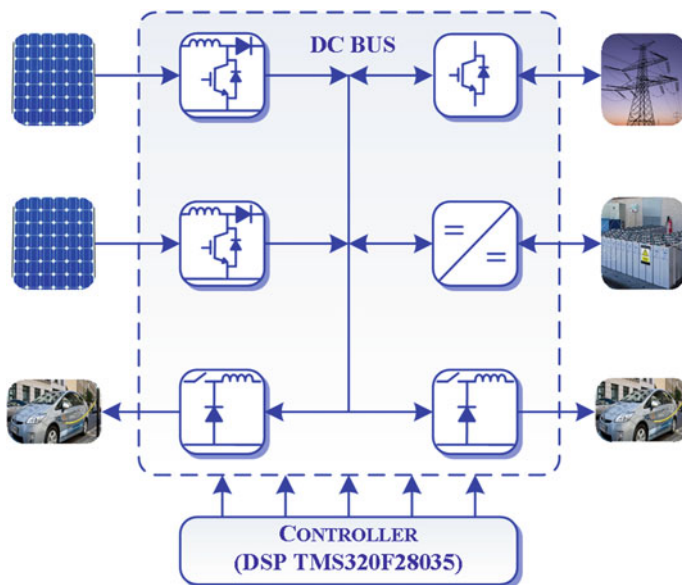


Fig. 2.7 Distributed architecture

at the docking station can be charged from two separate tracks i.e. using the energy from the VRLA batteries or the fuel cells. The use of storage capacity in PCFs has the following advantages [36]:

- Efficient use of renewable energy sources
- Maximization of renewable energy sources contribution
- Better demand and production match, better auxiliary service supply and improved overall reliability

The core idea of including an ESU (energy storage unit) is that the power demand by PEVs can be either supplied by the PV or the utility or through a local energy storage unit. Energy derived from the ESU can charge the PEVs during certain contingencies such as islanding condition without the availability of PV power. It facilitates the charging of PEVs using minimum energy from the grid. The charging station appears as a dc microgrid with local generation from the PV system, PEVs' as loads and battery bank representing the storage system.

C. Single stage conversion with Z-converter

The double stage conversion described in the above architectures is replaced by a single stage using a Z-converter [22] as shown in Fig. 2.8. It does not require an additional DC/DC converter for each charging spot and a single DC/DC converter is employed to provide galvanic isolation. The Z-converter has double modulation capability, and can shape the grid current while simultaneously regulating PEV battery charging. The unit can be employed for both power absorption and injection, with simultaneously controlled battery charging. This ensures close to unity power factor for all operating modes and power flow paths; achieving this with a single conversion stage can be considered a unique advantage of the Z-converter. Furthermore, this topology possesses inherent buck-boost capability, allowing increased voltage range on the PV or grid. Despite the single conversion stage, reliability, rather than efficiency or cost, is the strong point of the Z-topology. Also the single phase power processed by the Z-converter consists of 120 Hz double line frequency ripple. This ripple can be mitigated by placing an additional decoupling capacitor across the PV source which introduces possible deviation from perfectly constant power extraction at the PV panels.

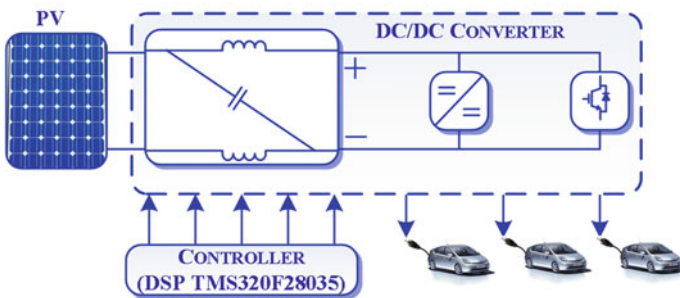


Fig. 2.8 Single stage conversion with Z-converter

2.5 Control Strategies

Workplace based photovoltaic charging facilities and residential PV charging are the two available options for charging PEVs using solar power. Depending on the solar irradiation, PEVs can be charged either from the photovoltaic or the distribution grid or both. The solar charging station should distribute the power available at the PV panels to the PEVs effectively and safely. Typically PEVs arrive at the charging facility with different State-of-Charge (SOC). More than often, the amount of PV power available to charge multiple PEVs is limited. Furthermore, the PV source is stochastic in nature, its power characteristic is nonlinear and the PEV batteries to be charged should be within certain voltage and current limits. Therefore, this process necessitates intelligent control of the power conditioning unit to manage the direction of power flow in PV integrated charging stations. Several algorithms have been proposed in the literature which differ significantly based on the type and location of the PCF. The algorithms also differ based on the various control parameters such as PV power, load demand, state-of-charge etc. Accordingly they can be classified as follows:

- A. Residential Photovoltaic Charging
- B. Battery Switch Stations
- C. Workplace Photovoltaic Charging

A. Residential Photovoltaic Charging

Few authors [37–40] have proposed an architecture for a grid-connected residential photovoltaic system that can be used to charge PEVs as well as to supply the existing household loads. The control algorithms depend on the power generated by the PV and the SOC of the PEV battery. Raul et al. [39] proposed a residential load coordination mechanism to charge PEVs. Depending on the load demand of the distribution transformers, the PEVs can be charged using renewable energy (PV/ Wind) or the power from the grid. Each household is installed with a rooftop PV system and a small scale wind turbine. A residential microgrid composed of rooftop panels and a biodiesel generator to charge PEVs and supply AC/DC household loads is described in [41]. In order to share the load among the sources, master-slave control method is employed. The operation of the residential microgrid depends on the PV power, load demand, SOC of the battery storage and tariff set by the utility. Most of the PEVs are not available for charging during daytime at residential facilities. Hence, this process demands for an additional component in the form of an energy storage unit which might not be economically attractive for an individual home owner. Residential charging is advantageous for households with more than one PEV.

B. Battery Switch Stations:

A PV based battery control strategy for charging multiple batteries in a solar battery charging station (SBCS) is proposed in [42]. The architecture of the SBCS is similar to the one shown in Fig. 2.6 but the DC/DC chargers are replaced by bi-directional switches. The proposed control strategy first charges each individual battery until

they reach the same voltage level and then charges the multiple batteries in parallel simultaneously according to the battery charging period and the available solar energy. This control strategy eliminates the use of multiple DC/DC converters per battery connection, making the SBCS less complicated and economical. Though being economical, the proposed architecture does not consider the scenarios when the PV panel is not generating any power or generating power in excess. Hence it cannot be considered for charging PEVs. A PV-based battery switch station (BSS) is proposed in [43]. The energy exchange strategy depends on the battery swapping demand of the PEVs and power generated by the PV. An algorithm is proposed to charge PEV batteries using the maximum energy from PV.

C. Workplace Photovoltaic Charging

In few cases, authors have proposed the idea of inserting a DC/DC battery charger at the dc link of the grid-connected PV system. By measuring the power generated by the PV and the power demand of the PEV, the control algorithm ensures the charging of the PEV battery from the appropriate source as described in [44]. Based on the imbalance between the PV power and the load demand, various possible scenarios are described. In case of [45], the power flow in a PV parking lot is managed through a set of computer controlled relays. PV panels of different ratings are interfaced with PEV chargers and the power grid through computer controlled relays. Depending on the irradiation levels, the relays direct the entire PV power to the PEVs or the grid or both. Hamilton et al. [46, 47] proposed an extension to this method for a modular dc PV charging station. Several PV panels are interfaced with the dc bus through a set of DC/DC converters. The DC/DC converter intelligently controls the power flow to the PEVs based on a certain preset limits of the dc bus voltage. Based on the preset limits the energy conversion unit facilitates three way energy flow among the power grid, PV modules and PEVs.

The concept of dc bus signalling has been proposed by several authors to schedule power to dc loads in a microgrid [48–50]. Few of them have extended this concept to charge PEVs in a microgrid environment [48, 49]. A smart charging station architecture integrated with PV power is proposed in [51, 52]. The smart charging station can operate in standalone mode and grid-connected mode. The switching between various modes is facilitated by the variation in dc link voltage levels induced due to the change in solar insolation. During the period of low solar insolation and peak load on distribution transformer, the controller shifts the charging of PEVs to non-peak period. The proposed control algorithm is simple as it involves only a single parameter i.e. dc link voltage to manage the direction of power flow in the charging station. It facilitates the charging of PEVs using minimum energy from the grid without any adverse impacts on the distribution transformer. The following sections explain the concept of dc link voltage sensing and its application for control and management of PV powered charging facilities.

2.5.1 Concept of DC Link Voltage Sensing

The primary requirement for a microgrid operation is to maintain the common dc bus voltage within an acceptable range. The terminals within a microgrid can be generally categorized into four types: generation, load, energy storage unit (ESU), and grid connection using voltage-source converters (VSCs). These four types of terminals can be further divided into two groups in terms of their contribution to system control and operation which are the power terminal and the slack terminal.

A power terminal is the one which outputs or absorbs power to/from the microgrid on its own and usually does not take the system's need into account. Typical examples would be variable dc loads (PEVs) and nondispatchable (variable) generation, such as wind turbines and photovoltaic based generations, when operating purely according to environmental conditions. Conversely, a slack terminal is the one which is responsible for balancing the power surplus/deficit caused by power terminals and maintaining stable system operation. Typical examples include a grid-connected VSC terminal (G-VSC) and ESU when they are actively supporting the dc microgrid system.

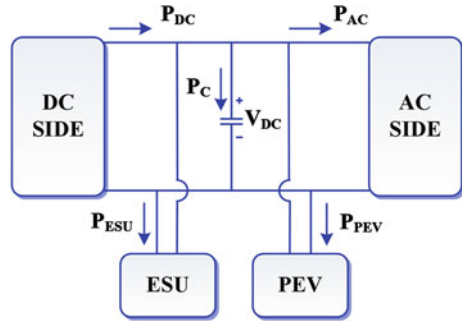
As previously described, different measures shall be taken by each terminal according to system operating conditions, thus a fast and reliable scheme for acknowledging system operation status is essential. Apart from using as communication means, dc link voltage is a good indicator of the system's operational status. The simplified equivalent circuit of the dc bus including the ESU and PEV is shown in Fig. 2.9, where P_{DC} and P_{AC} refer to the total power on the dc side (PV panel and DC/DC converter) and the ac side (inverter and the grid) of the dc bus respectively.

From Fig. 2.9, the instantaneous power relationship in a grid-connected PV system is given by

$$p_{dc}(t) = p_{ESU}(t) + p_c(t) + p_{PEV}(t) + p_{ac}(t) \quad (2.1)$$

where p_{dc} is the output power of the DC/DC converter on the dc side, p_{ESU} is the power delivered to (or by) the ESU, p_c is the power to the dc link capacitor, p_{PEV} is

Fig. 2.9 DC power flow



the power consumed by the plug-in electric vehicles, and p_{ac} is the power extracted by the inverter on the ac side. The instantaneous ac power (output of the inverter) can be written as

$$p_{grid}(t) = (V_m \sin \omega t)(I_m \sin \omega t) \quad (2.2)$$

$$= \frac{V_m I_m}{2} - \frac{V_m I_m}{2} \cos 2\omega t \quad (2.3)$$

where p_{grid} is the power injected into the grid, V_m is the amplitude of the phase voltage and I_m is the amplitude of the grid current. The ac power includes a dc term and a second-order ripple in the dc voltage. The average input power to the ac side can be written as

$$P_{AC} = V_{DC} I_{AC} \quad (2.4)$$

where I_{AC} is the average input current to the ac side (i.e. on the dc side of the inverter). Equating the average power on the input of ac side to the dc term on the output of ac side

$$\frac{V_m I_m}{2} = \eta V_{DC} I_{AC} \quad (2.5)$$

where η is the efficiency of the inverter. If V_{dc} and $V_{dc(ref)}$ are the actual and reference values of dc link voltage, respectively, the change in energy ΔE_{dc} stored in the dc link capacitor C_{dc} can be written as

$$\Delta E_{dc} = \frac{C_{dc}}{2} (V_{dc(ref)}^2 - V_{dc}^2) \quad (2.6)$$

To inject the PV power to the grid while maintaining a constant V_{dc} , the following energy balance should be satisfied:

$$\Delta E_{dc} = T(p_{dc} - p_{esu} - p_{PEV} - \frac{V_m I_m}{2\eta}) \quad (2.7)$$

where T is the time period of ac supply.

Combining (2.6) and (2.7)

$$V_{dc}^2 = V_{dc(ref)}^2 - \frac{2T}{C_{dc}} (p_{dc} - p_{PEV}) + \frac{2T}{C_{dc}} p_{dc} + \frac{2T}{C_{dc}\eta} V_m I_m \quad (2.8)$$

$$V_{dc} = \sqrt{V_{dc(ref)}^2 - \frac{2T}{C_{dc}} (p_{dc} - p_{PEV}) + \frac{2T}{C_{dc}} p_{ESU} + \frac{2T}{C_{dc}\eta} V_m I_m} \quad (2.9)$$

$$V_{dc} = \sqrt{V_{dc(ref)}^2 - \frac{2T}{C_{dc}}(\eta_{boost}P_{PV} - P_{PEV}) + \frac{2T}{C_{dc}}P_{ESU} + \frac{2T}{C_{dc}\eta}V_m I_m} \quad (2.10)$$

where η_{boost} is the efficiency of the DC/DC converter on the dc side.

From (2.10), it is clear that the fluctuations in PV power due to the change in solar irradiance causes variations in the dc link voltage. For a workplace based charging facility PEVs can be assumed to stay in the parking lot from morning till evening. Hence the variation in PEV load is considered.

Also from (2.7), the charging power of the dc capacitor can be written as

$$p_c = p_{dc} - p_{esu} - p_{PEV} - \frac{V_m I_m}{2\eta} \quad (2.11)$$

$$\frac{1}{2}cv_{dc}^2 = p_{dc} - p_{esu} - p_{PEV} - \frac{V_m I_m}{2\eta} \quad (2.12)$$

$$cv_{dc} \frac{dv_{dc}}{dt} = p_{dc} - p_{esu} - p_{PEV} - \frac{V_m I_m}{2\eta} \quad (2.13)$$

From 2.13, it can be inferred that a constant dc voltage indicates a balanced power flow among all the terminals, and a rising or dropping dc voltage indicates power surplus or deficit, respectively. Since the dc voltage can be used as an effective indicator of power-flow status, the control scheme of the proposed charging facility can be designed according to dc link voltage variation. Assuming the PEV demand to be constant over a period of time, the variation in dc link voltage occurs only due to the fluctuation in solar insolation. The operational voltage range can be divided into several levels. Based on the voltage level the charging facility has several modes of operation.

Figure 2.10 shows the variation in the dc link voltage and the power from the PV array with step changes in irradiation. A PV panel of rating 5.5 kW was modeled in Matlab taking the battery capacity of a single PEV into consideration. The reference dc link voltages have been chosen taking into consideration the change in sun conditions from early morning to late evening. As shown in Fig. 2.10 the PV array starts delivering power when the dc link voltage is greater than 50 V. At 250 V the PV system delivers 4,500 W which is the power requirement of standard PEV battery. Between 300 and 350 V the power delivered by the PV array is greater than 5,000 W, exceeding the power requirement of the PEV. This excess power can be sent to the grid. By taking the dc link voltage and the corresponding power delivered by the PV array into consideration, three reference voltage levels have been chosen as $V_{DC-1} = 50$ V, $V_{DC-2} = 250$ V and $V_{DC-3} = 350$ V. The modes of operation of the charging station are classified depending on the change in the dc link voltage. As the dc link voltage is the only criteria for switching between various modes the overall complexity of the system is reduced.

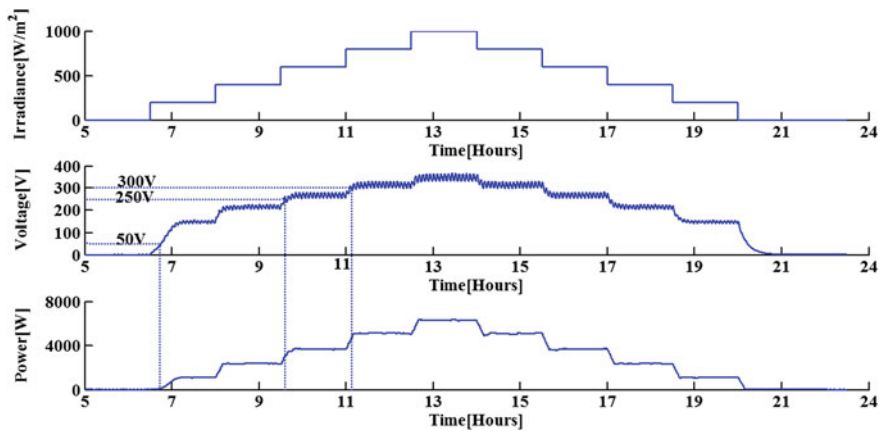


Fig. 2.10 Change in the dc link voltage and power generated by the PV with the change in sun condition

2.6 Power Management Algorithm for PV Charging Facility

The detailed circuit configuration for the proposed workplace based charging facility is shown in Fig. 2.11. The architecture consists of several strings of PV panels interfaced to their own DC/DC converters which share a common dc bus. The DC/DC boost converter performs the function of maximum power point tracking (MPPT) to facilitate the operation of PV panel at the maximum power point. The energy storage unit (ESU) is connected to the dc bus via a bi-directional DC/DC buck-boost converter. The ESU will support the charging of PEVs when there is no power available either from the grid or the PV. The battery pack in the ESU can be charged either from the grid during off peak hours or from the PV after all the PEVs have been charged in the charging facility. DC/DC buck converter connected to the dc bus controls the charging of the PEV. The control description shown for the charging facility in Fig. 2.11 is based on the requirements for two PEVs. Multiple PEVs can be charged by having separate buck converters installed for each charging point. The charging facility is connected to the power distribution network through a DC/AC bi-directional grid tied converter.

The control unit monitors and controls the power flow between the source and PEV. As shown in Fig. 2.11 the control unit generates the switching signals to control the various power converters in the charging facility based on the voltage and current values sensed by the voltage and current sensing units. V_{PV} , voltage across the PV array and I_{PV} , the current flowing from the PV array are used to implement MPPT by means of incremental conductance algorithm. V_{DC} is the magnitude of the voltage at the dc bus, V_{B1} and V_{B2} are the detected battery voltages of the PEVs which give a measure of the state-of-charge (SOC) while

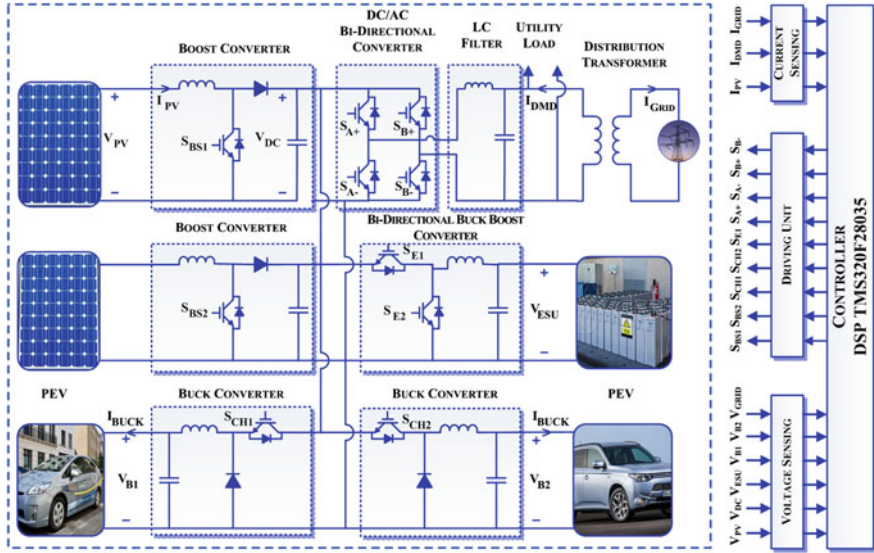


Fig. 2.11 Detailed circuit configuration of the proposed architecture

V_{ESU} gives the measure of the SOC of the ESU. I_{DMD} represents the loading condition of the distribution transformer, I_{grid} is the current fed into the grid by the DC/AC converter and V_{Grid} is the grid side voltage.

2.6.1 Modes of Operation

The operation of the charging station can be categorized into four modes: Mode-1 (grid-connected rectification), Mode-2 (PV charging and grid-connected rectification), Mode-3 (PV charging) and Mode-4 (grid-connected inversion). A set of variables I_{DMD} , $I_{DMD-max}$, V_{DC-1} , V_{DC-2} , V_{DC-3} , V_B and V_{BH} are used to describe the modes of operation. I_{DMD} represents the distribution transformer load and $I_{DMD-max}$ represents the peak load condition of the transformer. V_{DC} is the voltage at the dc bus. V_{DC-1} , V_{DC-2} and V_{DC-3} are the three chosen reference voltage levels of the dc bus. V_B and V_{ESU} are the detected battery voltages of the PEV and the ESU. V_{BH} is the battery voltage corresponding to the threshold value of the state-of-charge (T_{SOC}). The charging of PEV should be terminated once the battery voltage V_B is equal to V_{BH} . Figure 2.12 shows the direction of power flow during various modes of operation of the charging station.

The four modes of operation are described as follows:

Mode-1: $V_{DC} < V_{DC-1}$: Grid-connected rectification

Case-1: $V_{DC} < V_{DC-1}$ and $I_{DMD} < I_{DMD-max}$

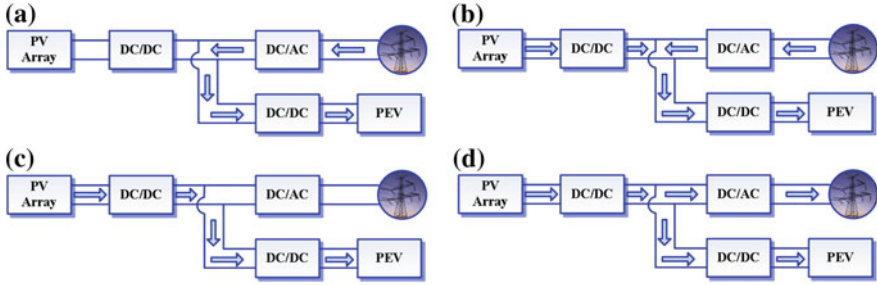


Fig. 2.12 Direction of power flow during the operation modes

In this mode the photovoltaic system does not generate any power either due to low radiation or bad weather conditions. The DC/DC boost converter is isolated and the power required to charge the PEV is provided by the grid. Anytime during this mode if the dc link voltage exceeds V_{DC-1} , the control shifts to Mode-2. The DC/DC buck converter regulates the output voltage to charge the PEV. As the grid is at off peak, it continues to supply power till the vehicle is completely charged. The controller terminates the charging of PEV by disabling the DC/DC buck converter when V_B exceeds V_{BH} and the grid supplies power to charge the battery pack in the ESU.

Case-2: $V_{DC} < V_{DC-1}$ and $I_{DMD} \geq I_{DMD-max}$

This mode is similar to Case-1 but with an increase in local demand on the distribution transformer. In order to reduce the stress on the grid, the charging of PEV is terminated temporarily by de-activating the grid-connected bi-directional DC/AC converter. As the distribution transformer is relieved from the additional burden of charging the PEV, it can continue supplying power to the local loads during the peak time. During this period the PEV can be charged by the ESU if the stored energy is sufficient to cater the needs of PEV charging. Once the grid is back to off peak condition (i.e. $I_{DMD} < I_{DMD-max}$) the charging of the PEV is restored and the controller monitors its charging.

Mode-2: $V_{DC-1} \leq V_{DC} < V_{DC-2}$: PV charging and grid-connected rectification

In this mode the power generated by the photovoltaic system is less than the power required to charge the PEV. Therefore all the power generated by the PV is transferred to the PEV and the deficit is supplied by the grid. The dc link voltage varies with the change in irradiation. This instantaneous change in the dc link voltage is sensed by the controller to generate an equal voltage at the output of the DC/AC bi-directional converter through the process of rectification. If at any point I_{DMD} exceeds $I_{DMD-max}$ the bi-directional DC/AC converter is isolated from the grid. The PV system continues charging the PEV whereas the grid caters the peak load demand.

Mode-3: $V_{DC-2} \leq V_{DC} < V_{DC-3}$: PV charging mode

In this mode the PV system generates all the power required to charge the PEV. As the grid does not supply any power it is isolated by the bi-directional DC/AC

converter. The controller ensures that the PEV is not over charged by terminating its charging once V_B exceeds V_{BH} (voltage corresponding to 95 % state of charge of the PEV battery). This mode occurs as long as the dc link voltage is in between V_{DC-2} and V_{DC-3} .

Mode-4: $V_{DC-link} \geq V_{DC-3}$: PV charging mode and Grid inversion mode

The PV array generates excess power once the dc link voltage exceeds V_{DC-3} . This additional power generated by the PV array is sent to the grid via the bi-directional DC/AC converter. Once the PEVs are charged, all the power from the PV source is sent to the grid. The mode then resembles normal operation of PV generation systems.

2.6.2 Control Description

2.6.2.1 DC/DC Boost Converter

The control method for DC/DC boost converter is summarized in Fig. 2.13. A single phase boost stage is used to boost the PV voltage and track the MPP of the panel. To track the MPP, input voltage (V_{PV}) and input current (I_{PV}) are sensed. The two values are then used by the MPPT algorithm. The MPPT is realized using an outer voltage loop that regulates the input voltage i.e. panel voltage by modulating the current reference for the inner current loop of the boost stage.

Two 2-pole 2-zero controllers, $G_V(S)$ and $G_I(S)$ are used to close the inner DC-DC boost current loop and the outer input voltage loop. MPPT algorithm provides reference input voltage, V_{MPPT} to the boost stage to enable panel operation at maximum power point. The sensed input voltage is compared with the voltage command (V_{MPPT}), generated by MPPT controller, in the voltage control loop. The voltage controller output, $I_{boostsw_Ref}$ is then compared with the output current ($I_{boostsw}$) feedback in the current controller. The current loop controller output determines the PWM duty cycle so as to regulate the input voltage indirectly.

2.6.2.2 DC/AC Inverter

The control method for grid-connected DC/AC converter is shown in Fig. 2.14. This stage uses two nested control loops—an outer voltage loop and an inner current loop. V_{dc_Ref} is the reference voltage for the DC link, V_{DC} is the detected

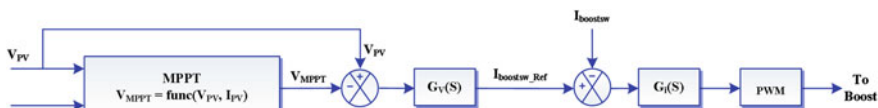


Fig. 2.13 Control diagram of DC/DC boost converter

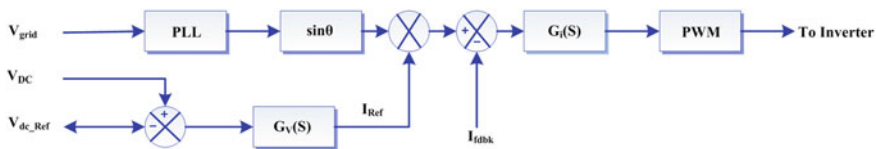


Fig. 2.14 Control diagram of DC/AC inverter

DC link voltage, V_{grid} is the voltage at the secondary of the distribution transformer, θ is the grid phase angle, I_{REF} is the reference current for the DC/AC converter generated by the voltage loop and I_{fdbk} is the current fed into the grid by the DC/AC converter.

Two PID controllers, $G_V(S)$ and $G_i(S)$ are used to close the outer voltage loop and the inner current loop. The voltage loop generates the reference command (I_{Ref}) for the current loop as increasing the current command will load the stage and hence cause a drop in the DC link voltage the sign for reference and the feedback are reversed. The current command is then multiplied by the AC angle to get the instantaneous current reference. Since the inverter is grid connected the grid angle is provided by the PLL. The instantaneous current reference is then used by the current compensator along with the feedback current (I_{fdbk}) to provide duty cycle for the full bridge inverter.

2.6.2.3 DC/DC Buck Converter

The control method for DC/DC buck converter for PEV charging is based on V_B , V_{BH} , I_{DMD} and $I_{DMD-max}$ as shown in Fig. 2.15. V_B is the detected battery voltage, V_{BH} is the battery voltage corresponding to 95 % SOC. I_{DMD} is the load on the distribution transformer and $I_{DMD-max}$ represents the peak load condition. The control mode is determined by the detected battery voltage of the PEV and the loading condition of the distribution transformer. The charging of the PEV is turned

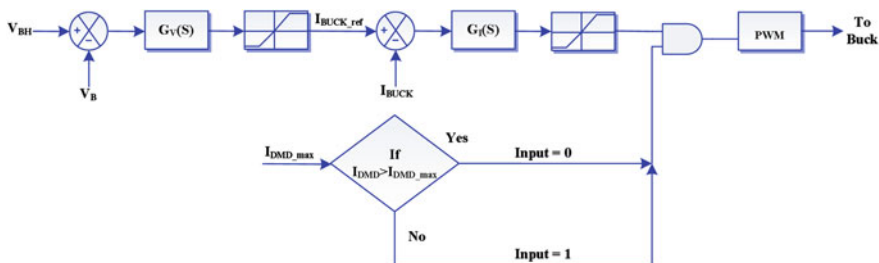


Fig. 2.15 Control diagram of DC/DC buck converter

off once the battery voltage reaches V_{BH} or the distribution transformer reaches the peak load condition.

2.6.3 Simulation Studies

In order to validate the proposed control algorithm simulations were done in Matlab Simulink using the simpowersystems toolbox. The reference dc bus voltages i.e. V_{DC-1} , V_{DC-2} and V_{DC-3} are set at 50, 250 and 350 V. The reference dc link voltage levels are selected based on a training mode wherein the PEV load is kept constant and the solar irradiation is allowed to vary in steps. The values of $I_{DMD-max}$ and T_{soc} are set at 80 A (peak to peak) and 95 %. Toyota Prius plug-in hybrid has been chosen as the PEV which has a total battery capacity equal to 4.5 kWh and nominal voltage equal to 48 V. The rms value of AC grid voltage is 240 V. A PV panel of rating 5.5 kW has been modelled taking the battery capacity of the PEV into consideration. The reference dc bus voltages have been chosen taking into consideration the change in sun conditions from early morning to late evening (Fig. 2.10). As the dc bus voltage varies, the source from which the PEV is charged also varies accordingly. Simulation results describing the transitions between various modes are shown below.

Figure 2.16 shows the transition of the grid from off peak to on peak when the charging station is operating in mode 1. The loading condition is accessed by measuring the current (I_{DMD}) on the secondary side of the distribution transformer. Initially the grid is at off peak and hence the AC grid delivers the power required to charge the PEV and other local loads. As shown in Fig. 2.16, from 1.5 to 2.0 s the

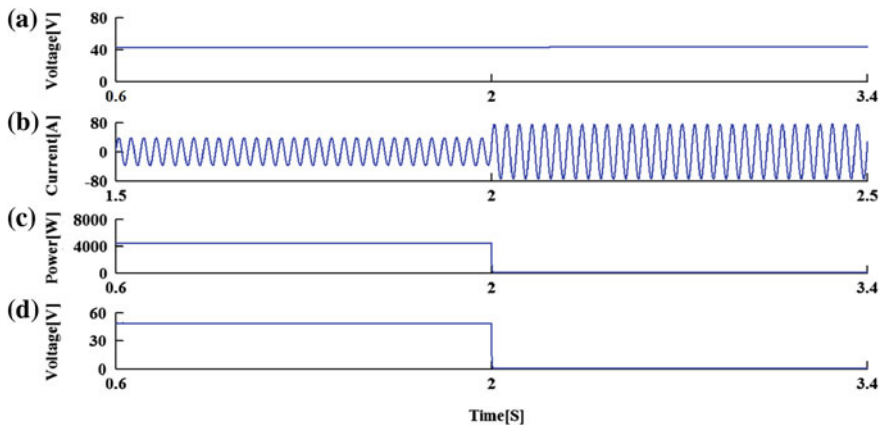


Fig. 2.16 Matlab simulink outputs for transition from mode-1 case-2. **a** DC bus voltage. **b** Current flowing from the distribution transformer to the loads and the PEV. **c** Power delivered to the PEV (charging power). **d** Output voltage of the DC/DC buck converter

current flowing in the secondary side of the distribution transformer is less than 80 A. With the increase in utility load at 2.0 s, I_{DMD} exceeds 80 A ($I_{DMD-max}$). The charging of the PEV is terminated when the current flowing from the distribution transformer, I_{DMD} exceeds $I_{DMD-max}$. This is done to reduce the stress being imposed on the AC grid during the peak time. Hence the power consumed by the PEV reduces to zero during the peak time as shown in the figure.

The simulation results for the transition from mode 2 to mode 3 are shown in Fig. 2.17. During the initial stages the dc bus voltage is less than 250 V and grid continues to supply the deficit power to charge the PEV. Once the dc bus voltage exceeds 250 V, the PV system alone caters the charging of PEV. The power flowing from the PV and the Power Grid is shown in Fig. 2.17. As shown in the figure, the deficit power of 1,000 W to charge the PEV is supplied by the grid in mode-2 and it does not supply any power in mode-3 as the PV alone caters to the demand of the PEV.

The transition from mode 3 to mode 4 is shown in Fig. 2.18. With the dc bus voltage exceeding 350 V there is an increase in power flowing from the PV in mode 4. The PV system feeds this excess power to the grid in addition to charging the PEV. The sinusoidal output of the DC/AC bi-directional converter shows that it acts as an inverter in this case. In order to maintain the energy balance the dc link voltage is kept constant at 360 V. Finally Fig. 2.19 shows the termination of the vehicle charging when $SOC = T_{soc}$.

The simulation results validate the modes of operation and the control algorithm described in this section. As described in Sect. 1.5.1, the modes of operation change due to the change in the dc bus voltage which in turn changes due to the change in the irradiation levels according to the time of the day.

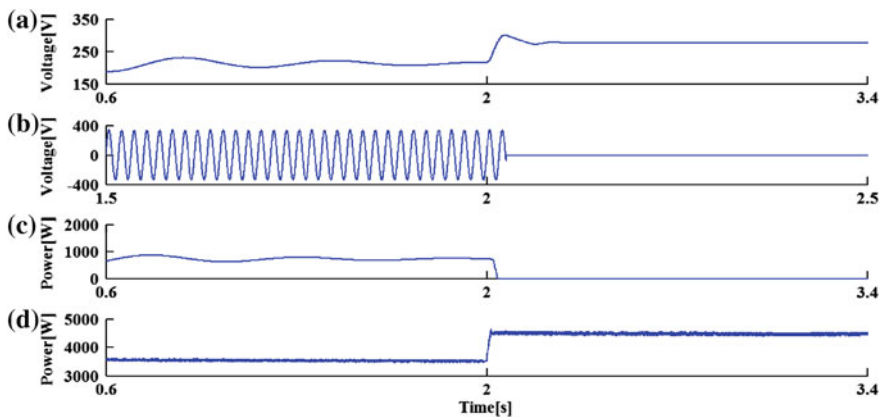


Fig. 2.17 Matlab simulink outputs for transition from mode 2 to mode 3. **a** DC bus voltage. **b** Voltage of the grid. **c** Power delivered by the grid. **d** Power delivered by the PV array

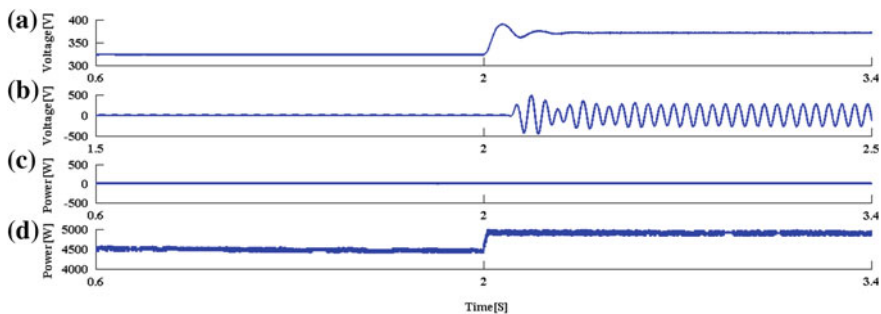


Fig. 2.18 Matlab simulink outputs for transition from mode 3 to mode 4. **a** DC bus voltage. **b** Output voltage of the DC/AC bi-direction converted (inverter). **c** Power delivered by the grid. **d** Power delivered by the array

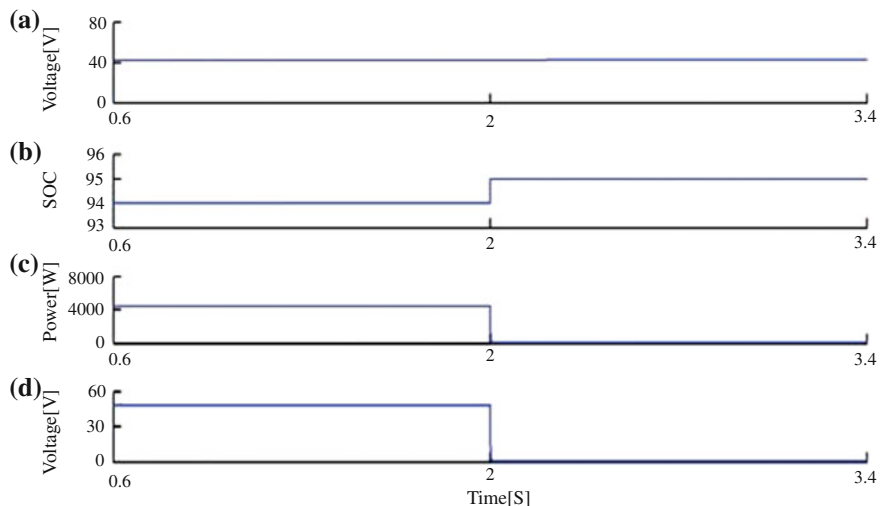


Fig. 2.19 Matlab simulink outputs for transition in state-of-the-charge during mode-1. **a** DC bus voltage. **b** State-of-charge of the PHEV battery. **c** Charging power delivered to the PHEV. **d** Output voltage of the DC/DC buck converter

2.6.4 Experimental Verification

To verify the practical feasibility and effectiveness of the proposed control strategies experimental tests have been carried out in the laboratory. C2000 microcontroller, TMS320F28035 by TI (Texas Instruments) is used to generate all the required control signals.

Figure 2.20 shows the experimental setup of the system. The components include the Solar Explorer Kit by TI (Texas Instruments), power pole board in buck configuration by Hirel, an isolation transformer and a battery. The DC/DC boost

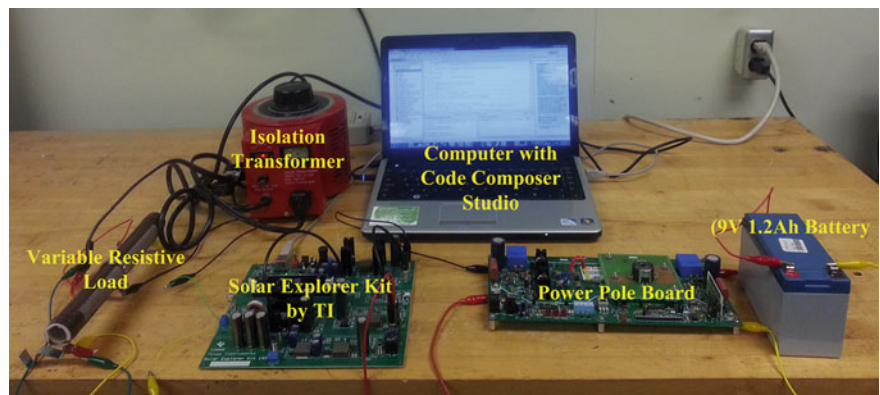


Fig. 2.20 Experimental setup

converter for the PV stage and the inverter is a part of the solar explorer kit; and the DC/DC buck converter for PEV charging is the Power-Pole board from Hirel. A synchronous buck boost stage which is integrated on the board (solar explorer kit) is used to emulate the PV panel. In the place of a PEV a 9 V 1,200 mAh battery is used. By changing the value of irradiation different modes of operation are emulated. Since this is a scaled down version the dc link reference voltage levels are chosen as $V_{DC-1} = 15\text{ V}$, $V_{DC-2} = 20\text{ V}$ and $V_{DC-3} = 25\text{ V}$. The value of $I_{DMD-max}$ is chosen as 1.5 A. Depending on the reference voltage levels the different modes of operation are classified as follows:

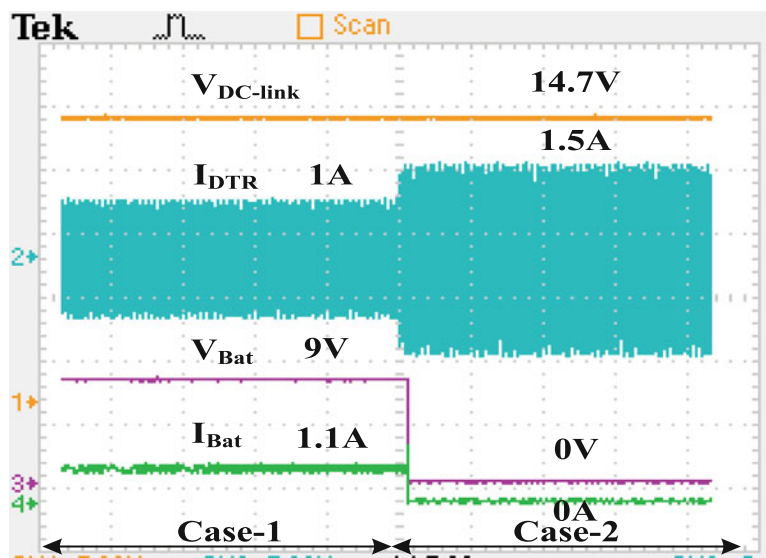


Fig. 2.21 Experimental outputs describing the loading of distribution transformer in Mode-1

$$\begin{aligned}
 V_{dc-Link} &< 15 \text{ V} - \text{Mode-1} \\
 15 \text{ V} &< V_{dc-Link} < 20 \text{ V} - \text{Mode-2} \\
 20 \text{ V} &< V_{dc-Link} < 25 \text{ V} - \text{Mode-3} \\
 V_{dc-Link} &> 25 \text{ V} - \text{Mode-4}
 \end{aligned}$$

Experimental tests have been carried out in terms of steady-state performance and transient-performance between different modes and the results are provided below. Figure 2.21 through 2.25 explain the experimental results for the various modes of operation.

Experimental results for Mode-1 are shown in Fig. 2.21. With the increase in the loading of distribution transformer, I_{DMD} increases from 1 to 1.5 A as shown in Fig. 2.21 and accordingly the PEV is turned off so that the grid can cater to other loads without overloading the distribution transformer (assuming that $I_{DMD-max} = 1.5 \text{ A}$). The turning-off of the PEV is illustrated by the fact that V_B and I_B go to zero with the increase in distribution transformer loading. This is done by generating a duty cycle of zero for the buck converter switch.

Experimental results for the transition between Mode-2 and Mode-3 are shown in Fig. 2.22. In the initial state, the dc link voltage is around 15.7 V and current flows from both the PV as well as the grid to charge the PEV. Once the dc link voltage increases to 22.4 V (Mode-3) no power is drawn from the grid.

Transition from Mode-3 to Mode-4 is shown in Fig. 2.23. With the change in dc link voltage from 22.4 to 29.9 V the bi-directional converter goes from off-state to

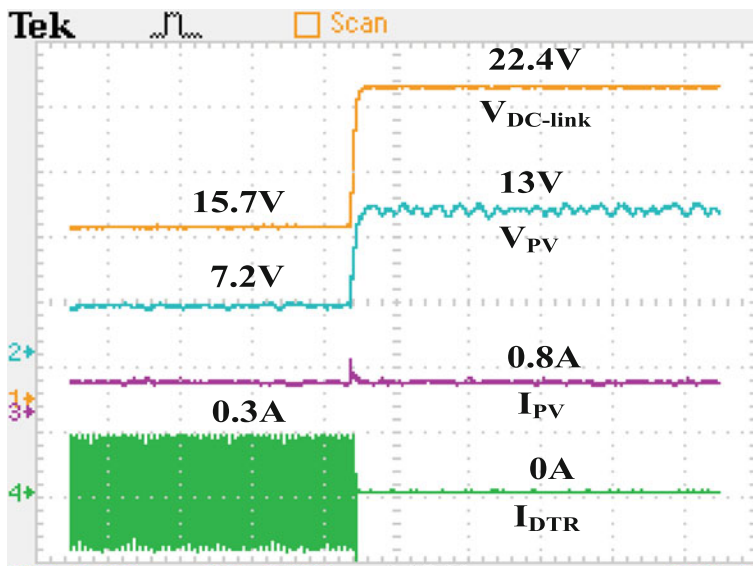


Fig. 2.22 Experimental outputs for transition from Mode-2 to Mode-3

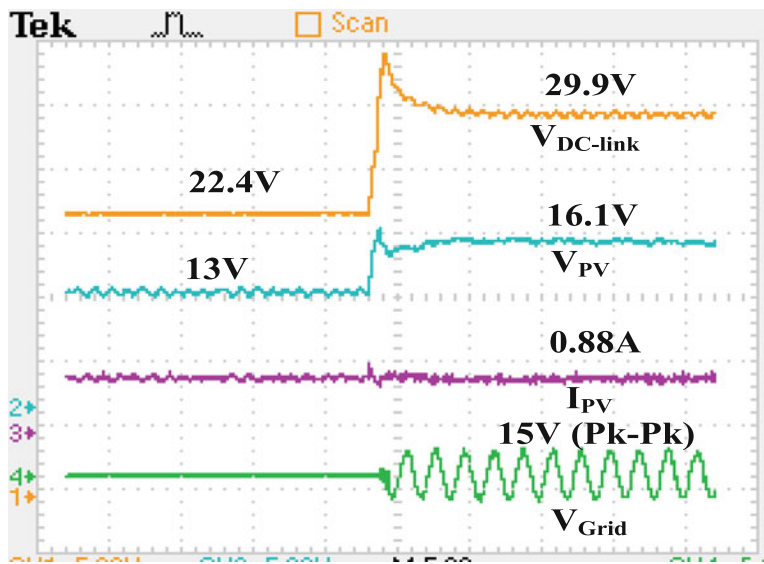


Fig. 2.23 Experimental outputs for transition from Mode-3 to Mode-4

on-state. Mode-4 resembles the normal operation of a grid connected PV system. In this case the battery has been completely charged and hence the entire power generated by the PV is delivered to the grid. Figure 2.24 shows the steady state experimental results of Mode-4. The dc link voltage is 29.9 V and the output

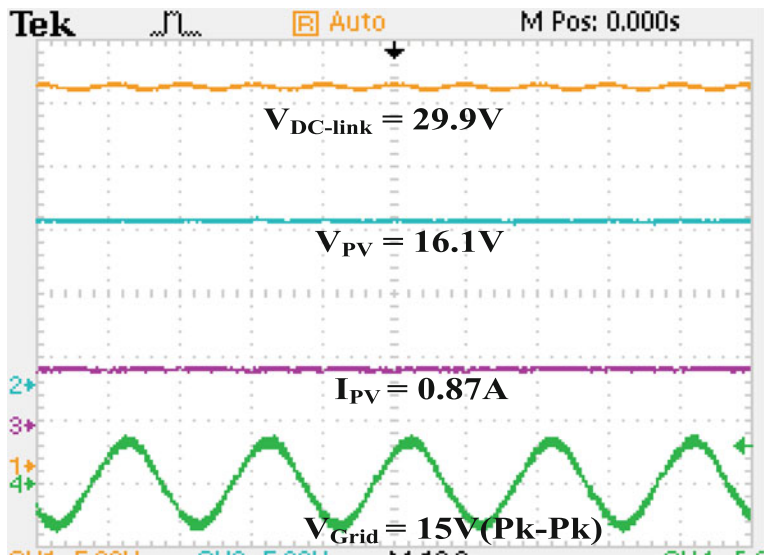


Fig. 2.24 Experimental outputs Mode-4

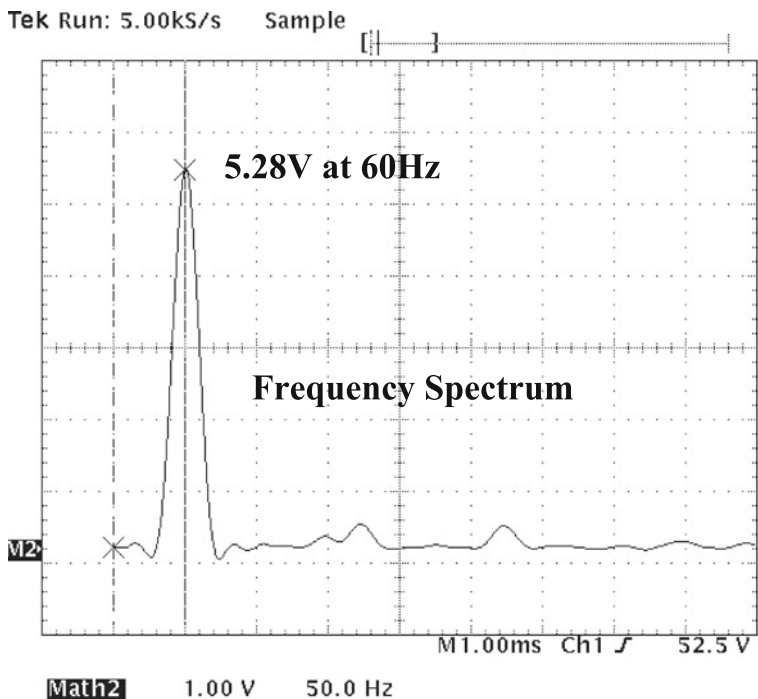


Fig. 2.25 FFT of inverter output voltage

voltage of the inverter is a sine wave. A high switching frequency along with LCL filter meets the total harmonic distortion (THD) requirements. Unipolar switching strategy was followed for inverter switching and the switching takes place at 20 kHz. The inverter switching at 20 kHz together with the LCL filter generates a filtered single phase AC output. The total harmonic distortion (THD) of the inverter output voltage is calculated to be 5.4 %. Figure 2.25 shows the Fast Fourier Transform (FFT) of the inverter output voltage.

2.7 Conclusion

To mitigate the loading on distribution transformers due to PEV charging, smart charging strategies coupled with renewable energy resources are the need of the hour. This chapter discussed the current state of the infrastructure for PV powered charging facilities for PEVs. Several power electronic topologies are presented and compared. Control strategies are reviewed for residential and workplace based photovoltaic charging. The chapter proposed a charging station architecture based on distributed topology. A unique control strategy based on dc link voltage sensing, which decides the direction of power flow is presented and the various modes of

operation have been described. The practical feasibility and effectiveness of the proposed control strategy has been validated by simulation and experimental results. The proposed control method based on the change in dc link voltage level due to the change in irradiation of the sun, is simple and unique. The energy management algorithm facilitates charging of the PEVs using minimum energy from the utility with a kind of demand management to improve the energy efficiency. Smart charging techniques like the one proposed in this chapter will help avoid major expense to upgrade distribution transformers and other substation equipment with the increase in PEV loads on the distribution system.

References

1. Kempton W, Tomic J (2005) Vehicle-to-grid power implementation: from stabilizing the grid to supporting large-scale renewable energy. *J Power Sources* 144(1):280–294
2. EPRI (2012) Tennessee valley authority smart modal area recharge terminal (SMART) station project. <http://www.epri.com/abstracts/Pages/ProductAbstract.aspx?ProductId=000000000001026583>. Accessed Nov 2012
3. Gorton M (2011) Solar-powered electric vehicle charging stations sprout up nationally. <http://www.renewableenergyworld.com/rea/news/article/2011/11/solar-powered-electric-vehicle-charging-stations-sprout-up-nationally>. Accessed Nov 2011
4. Motavalli J (2013) Here now: the world's first portable, self-contained solar EV charging station. <http://www.plugincars.com/here-now-worlds-first-portable-self-contained-solar-ev-charging-station-128015.html>. Accessed Aug 2013
5. Ayre J Solar-integrated EV fast charging station (eco station) gets CODA energy storage system. <http://cleantechnica.com/2013/09/02/solar-integrated-ev-fast>
6. Giges NS (2012) Wind-powered charging stations coming soon. <https://www.asme.org/engineering-topics/articles/renewable-energy/wind-powered-charging-stations-coming-soon>. Accessed Oct 2012
7. Liu K, Makaran J (2009) Design of a solar powered battery charger. In: Electrical power and energy conference (EPEC), 22–23 Oct 2009
8. Neumann H, Schar D, Baumgartner F (2012) The potential of photovoltaic carports to cover the energy demand of road passenger transport. *Prog Photovolt Res Appl* 20:639–649
9. Ingersoll JG, Perkins CA (1996) The 2.1 kW photovoltaic electric vehicle charging station in the city of Santa Monica, California. In: The twenty fifth IEEE photovoltaic specialists conference, 13–17 May 1996
10. Locment F, Sechilariu M, Forgez C (2010) Electric vehicle charging system with PV grid-connected configuration. In: IEEE vehicle power and propulsion conference (VPPC), 1–3 Sept 2010
11. Letendre S (2009) Solar electricity as a fuel for light vehicles. In: Proceedings of the 2009 American solar energy society annual conference, Boulder, CO
12. Tulpule PJ, Marano V, Yurkovich S, Rizzoni G (2013) Economic and environmental impacts of a PV powered workplace parking garage charging station. *J Appl Energy* 108:323–332
13. Birnie III DP (2009) Solar-to-vehicle (S2 V) systems for powering commuters of the future. *J Power Sources* 186(2):539–542
14. Zhang Q, Tezuka T, Ishihara KN, Mclellan BC (2012) Integration of PV power into future low-carbon smart electricity systems with EV and HP in Kansai Area, Japan. *J Renew Energy* 44:99–108
15. Denholm P, Kuss M, Margolis RM (2012) Co-benefits of large scale plug-in hybrid electric vehicle and solar PV deployment. *J Power Sources* 236:350–356

16. National Household Travel Survey (NHTS) (2009). Summary of travel trends-2009. <http://nhts.orl.gov/2009/pub/stt.pdf>. Accessed Oct 2009
17. Rutherford MJ, Yousefzadeh V (2011) The impact of electric vehicle battery charging on distribution transformers. In: Twenty-sixth annual IEEE applied power electronics conference and exposition (APEC), 2011
18. Green RC, Wang L, Alam M (2011) The impact of plug-in hybrid electric vehicles on distribution networks: a review and outlook. *J Renew Sustain Energy Rev* 15(1):544–553
19. Shao SN, Pipattanasomporn M, Rahman S (2009) Challenges of PHEV penetration to the residential distribution network. In: IEEE power and energy society general meeting, 26–30 July 2009
20. Zhao J, Kucuksari S, Mazhari E, Son YJ (2013) Integrated analysis of high-penetration PV and PHEV with energy storage and demand response. *J Appl Energy* 112:35–51
21. Erol-Kantarci M, Mouftah H (2011) Management of PHEV batteries in the smart grid towards a cyber-physical power infrastructure. In: IEEE workshop on design, modeling and evaluation of cyber physical systems, July 2011
22. Carli G, Williamson SS (2013) Technical considerations on power conversion for electric and plug-in hybrid electric vehicle battery charging in photovoltaic installations. *IEEE Trans Power Electron* 28(12):5784–5792
23. Giannouli M, Yianoulis P (2012) Study on the incorporation of photovoltaic systems as an auxiliary power source for hybrid and electric vehicles. *J Sol Energy* 86(1):441–451
24. Li X, Lopes LAC, Williamson SS (2009) On the suitability of plug-in hybrid electric vehicle (PHEV) charging infrastructures based on wind and solar energy. In: IEEE power and energy society general meeting, 26–30 July 2009
25. Hadley, SW (2007) Evaluating the impact of plug-in hybrid electric vehicles on regional electricity supplies. In: Bulk power system dynamics and control—VII. Revitalizing operational reliability, Aug 2007
26. Yan Q, Kezunovic M (2012) Impact analysis of electric vehicle charging on distribution system. In: North American power symposium (NAPS), Sept 2012
27. Moghe R, Kreikebaum F, Hernandez JE, Kandula RP, Divan D (2011) Mitigating distribution transformer lifetime degradation caused by grid-enabled vehicle (GEV) charging. In: IEEE energy conversion congress and exposition (ECCE), Sept 2011
28. Masoum AS, Deilami S, Moses PS, Abu-Siada (2010) A impacts of battery charging rates of plug-in electric vehicle on smart grid distribution systems. In: IEEE PES innovative smart grid technologies conference Europe (ISGT Europe), Oct 2010
29. Qian K, Zhou C, Allan M, Yuan Y (2010) Load model for prediction of electric vehicle charging demand. In: International conference on power system technology (POWERCON), Oct 2010
30. Papadopoulos P, Skarvelis-Kazakos S, Grau I, Cipcigan LM, Jenkins N (2010) Predicting electric vehicle impacts on residential distribution networks with distributed generation. In: IEEE vehicle power and propulsion conference (VPPC), Sept 2010
31. Jian L, Xue H, Xu G, Zhu X, Zhao D, Shao Z (2013) Regulated charging of plug-in hybrid electric vehicles for minimizing load variance in household smart microgrid. *IEEE Trans Industr Electron* 60(8):3218–3226
32. Osawa M, Yoshimi K, Yamashita D, Yokoyama R, Masuda T, Kondou H, Hirota T (2012) Increase the rate of utilization of residential photovoltaic generation by EV charge-discharge control. In: IEEE innovative smart grid technologies—Asia (ISGT Asia), May 2012
33. Chukwu UC, Mahajan SM (2014) V2G parking lot with pv rooftop for capacity enhancement of a distribution system. *IEEE Trans Sustain Energy* 5(1):119–127
34. Geiles TJ, Islam S (2013) Impact of PEV charging and rooftop PV penetration on distribution transformer life. In: IEEE power and energy society general meeting (PES), 21–25 July 2013
35. Robalino DM, Kumar G, Uzoehi LO, Chukwu UC, Mahajan SM (2009) Design of a docking station for solar charged electric and fuel cell vehicles. In: International conference on clean electrical power, 9–11 June 2009

36. Alamri BR, Alamri AR (2009) Technical review of energy storage technologies when integrated with intermittent renewable energy. In: International conference on sustainable power generation and supply, SUPERGEN, 6–7 April 2009
37. Gurkaynak Y, Khaligh A (2009) Control and power management of a grid connected residential photovoltaic system with plug-in hybrid electric vehicle (PHEV) load. In: Twenty-fourth annual IEEE applied power electronics conference and exposition (APEC), 15–19 Feb 2009
38. Nagarajan A, Shireen W (2010) Grid connected residential photovoltaic energy systems with plug-in hybrid electric vehicles (PHEV) as energy storage. In: IEEE power and energy society general meeting, 25–29 July 2010
39. Oviedo RM, Fan Z, Gormus S, Kulkarni P (2014) A residential PHEV load coordination mechanism with renewable sources in smart grids. *J Electr Power Energy Syst* 55:511–521
40. Gurkaynak Y, Li Z, Khaligh A (2009) A novel grid-tied, solar powered residential home with plug-in hybrid electric vehicle (PHEV) loads. In: IEEE vehicle power and propulsion conference VPPC 09, 7–10 Sept 2009
41. Roggia L, Rech C, Schuch L, Baggio JE, Hey HL, Pinheiro JR (2011) Design of a sustainable residential microgrid system including PHEV and energy storage device. In: Proceedings of the 2011—14th European conference on power electronics and applications (EPE 2011), 30 Aug–1 Sept 2011
42. Sheng S, Hsu CT, Li P, Lehman B (2013) Energy management for solar battery charging station. In: IEEE 14th workshop on control and modeling for power electronics (COMPEL), 23–26 June 2013
43. Chen Z, Liu N, Xiao X, Lu X, Zhang J (2013) Energy exchange model of PV-based battery switch stations based on battery swap service and power distribution. In: IEEE vehicle power and propulsion conference (VPPC), Oct 2013
44. Choe GY, Kim JS, Lee BK, Won CY, Lee TW (2010) A bi-directional battery charger for electric vehicles using photovoltaic PCS systems. In: IEEE vehicle power and propulsion conference (VPPC), 1–3 Sept 2010
45. Vaidya M, Stefanakos EK, Krakow B, Lamb HC, Arbogast T, Smith T (1996) Direct DC-DC electric vehicle charging with a grid connected photovoltaic system. In: Twenty fifth IEEE photovoltaic specialists conference, 13–17 May 1996
46. Gamboa G, Hamilton C, Kerley R, Elmes S, Arias A, Shen J, Batarseh I (2011) Control strategy of a multi-port, grid connected, direct-DC PV charging station for plug-in electric vehicles. In: IEEE energy conversion congress and exposition (ECCE), 12–16 Sept 2011
47. Hamilton C, Gamboa G, Elmes J, Kerley R, Arias A, Pepper M, Shen J, Batarseh I (2010) System architecture of a modular direct-DC PV charging station for plug-in electric vehicles. In: 36th annual conference on IEEE industrial electronics society (IECON), 7–10 Nov 2010
48. Schönberger J, Duke R, Round SD (2006) DC-Bus signaling: a distributed control strategy for a hybrid renewable nanogrid. *IEEE Trans Industr Electron* 53(5):1453–1460
49. Sun K, Zhang L, Xing Y, Guerrero JM (2011) A distributed control strategy based on dc bus signaling for modular photovoltaic generation systems with battery energy storage. *IEEE Trans Power Electron* 26(10):3032–3045
50. Jin C, Wang P, Xiao J, Tang Y, Choo FH (2014) Implementation of hierarchical control in DC microgrids. *IEEE Trans Industr Electron* 61(8):4032–4042
51. Preetham G, Shireen W (2012) Photovoltaic charging station for plug-in hybrid electric vehicles in a smart grid environment. Paper presented at IEEE PES innovative smart grid technologies, 16–20 Jan 2012
52. Goli P, Shireen W (2014) PV integrated smart charging of PHEVs based on DC link voltage sensing. *IEEE Trans Smart Grid* 5(3):1421–1428

<http://www.springer.com/978-981-287-316-3>

Plug In Electric Vehicles in Smart Grids

Charging Strategies

Rajakaruna, S.; Shahnian, F.; Ghosh, A. (Eds.)

2015, IX, 326 p. 164 illus., 109 illus. in color., Hardcover

ISBN: 978-981-287-316-3